

## Photoemission Extended Fine Structure Study of the SiO<sub>2</sub>/Si(111) Interface

M. T. Sieger,\* D. A. Luh, T. Miller, and T.-C. Chiang<sup>†</sup>

*Department of Physics, University of Illinois at Urbana-Champaign, 1110 West Green Street, Urbana, Illinois 61801-3080*  
*and Seitz Materials Research Laboratory, University of Illinois at Urbana-Champaign, 104 South Goodwin Avenue,*  
*Urbana, Illinois 61801-2902*

(Received 11 March 1996)

High-resolution Si 2*p* core level photoemission spectra of the SiO<sub>2</sub>/Si(111) system show chemically shifted components derived from individual oxidation states, which exhibit strong intensity modulations as a function of photon energy due to final-state diffraction. Analysis of these photoemission intensity modulations gives bond-length information specific to the individual suboxide. The results indicate that the interface is atomically abrupt. [S0031-9007(96)01259-8]

PACS numbers: 68.35.Bs, 79.60.Dp

The structure of SiO<sub>2</sub>/Si interfaces is a topic of great interest because of the ubiquity of SiO<sub>2</sub>/Si structures in semiconductor devices, and because, despite years of study, a detailed understanding of the interface structure is still lacking [1]. Although the large lattice mismatch between Si and SiO<sub>2</sub> disallows significant epitaxial and single-crystalline growth [2], there are surprisingly few electrical defects at the interface, resulting in a nearly ideal electrical behavior. An issue of central importance to the ongoing discussion of the interface structure concerns the chemical abruptness of the interface. While suboxides are necessarily present in the transition region from Si to SiO<sub>2</sub>, the question is whether or not this transition occurs with an atomically sharp boundary. Of all the major experimental tools that have been employed in such studies, high-resolution photoemission is the only technique that allows the distinction of individual oxidation states of Si (Si<sup>0</sup>, Si<sup>1+</sup>, Si<sup>2+</sup>, Si<sup>3+</sup>, and Si<sup>4+</sup>) by their chemical shifts [1,3–5], but its implementation so far has been unable to make a direct link between the observed chemical states and the interface structure.

The present work is an application of extended fine structure analysis to high-resolution photoemission from the SiO<sub>2</sub>/Si(111) interface. Photoemission extended fine structure (PEFS) is a well known technique, which can provide an accurate measure of local atomic bond lengths [6–8]. In our study, this analysis is applied to individual oxidation states of Si as observed by Si 2*p* core level photoemission. Our measurements show that final-state diffraction effects are significant, resulting in considerable modulation of the photoemission intensity as the excitation energy is varied. This diffraction fine structure at the SiO<sub>2</sub>/Si(111) interface has not been observed before, to our knowledge, and yields detailed information about the local bonding structure of each resolved Si oxidation state. Our analysis of the local bond lengths leads to the conclusion that the SiO<sub>2</sub>/Si(111) interface is chemically abrupt, with the intermediate oxidation states confined to the interface monolayer.

Thin (~10 Å) SiO<sub>2</sub> films were grown *in situ* by exposing clean Si(111)-(7 × 7) substrates to pure O<sub>2</sub> at a pressure of 5 × 10<sup>-8</sup> torr for 2000 s, with the samples held at 600 °C during exposure. Heating was accomplished by passing a current directly through the sample. The photoemission spectra were taken at the University of Wisconsin's Synchrotron Radiation Center (Stoughton, Wisconsin). The data were acquired with a hemispherical electron energy analyzer with an acceptance cone of about 7 × 13 deg, with the cone axis perpendicular to the surface. The linearly polarized photon beam was in grazing incidence, with its polarization vector ~3° to the surface normal and pointed into the analyzer. The *z* axis for the system is defined to be the sample normal.

Figure 1 shows a representative photoemission spectrum of the oxidized Si(111) surface and its decomposition into constituent components. As is known from previous studies [1,3–5], the line shape consists of five components, corresponding to bulk Si and the four oxidation states Si<sup>1+</sup>–Si<sup>4+</sup> (labeled S1–S4). Each component consists of a pair of spin-orbit split peaks. The spectral parameters for the line shapes are listed in Table I, which were deduced from an extensive analysis involving over

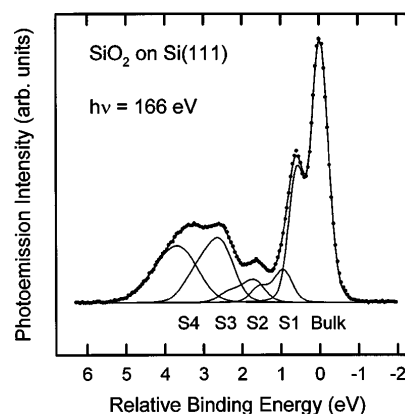


FIG. 1. A representative Si 2*p* core-level photoemission spectrum for SiO<sub>2</sub>/Si(111). The circles are data points, and the curves show a fit and the decomposition into components.

TABLE I. Fitting parameters for the Si  $2p$  core level spectra. Values are averages over many photon energies, except where noted. Quoted errors are one standard deviation. The  $\Delta$  width parameter is the difference between the oxide component Gaussian width and the bulk Gaussian width. All energies are in eV.

Fit parameter	Value
Spin-orbit splitting	0.61
Lorentzian full width	0.07
Branching ratio	$0.50 \pm 0.01$
S1 shift	$0.97 \pm 0.02$
S2 shift	$1.73 \pm 0.04$
S3 shift	$2.58 \pm 0.01$
S4 shift	$3.57 \pm 0.02$
Bulk Gaussian full width at $h\nu = 160$ eV	0.46
S1 $\Delta$ width	$0.02 \pm 0.01$
S2 $\Delta$ width	$0.07 \pm 0.02$
S3 $\Delta$ width	$0.13 \pm 0.01$
S4 $\Delta$ width	$0.25 \pm 0.02$

100 spectra taken at different photon energies and on different samples. The uncertainties shown in the table reflect the root mean square deviations from the mean, and our results are in good accord with previous studies [1,3–5]. All five components have the same line shape in our analysis, except that the Gaussian width becomes progressively larger for higher oxidation states. This broadening can be attributed to the increasing local disorder in going from pure Si to a nominally amorphous  $\text{SiO}_2$  film.

Figure 2 shows the photoemission intensities of the bulk component and S2–S4 components as a function of the excitation photon energy. As seen in Fig. 1, the S2–S4 components give rise to well defined peaks, while there are no obvious spectral features that can be associated with S1, due partly to its proximity to the much more intense bulk component. As a result, the S1 intensity cannot be reliably deduced, and is therefore excluded from our analysis. The curves in Fig. 2 show large intensity modulations due to diffraction in the final state, and there are significant differences among the curves. The oscillations are due primarily to backscattering from nearest neighbors located directly beneath the emitters [6–8]. Since the photoelectron final state has primarily  $d$  symmetry and the photon polarization vector is normal to the surface, the emission peaks along  $\theta = 0$  and  $\pi$ , which imparts a degree of sensitivity in our measurement to scatterers located above and below the emitter, on the  $z$  axis. This  $z$ -axis sensitivity is greatly enhanced by the angular dependence of the scattering amplitude. It is well known that the electron-atom scattering amplitude is strongly peaked in the forward-scattering and backscattering directions in this energy range. Any sidescattering from nearest neighbors not on the  $z$  axis must necessarily involve a scattering event with a relatively small amplitude compared to backscattering or forward scattering in order to interfere with the direct wave at the detector. Since forward scattering results in no geometri-

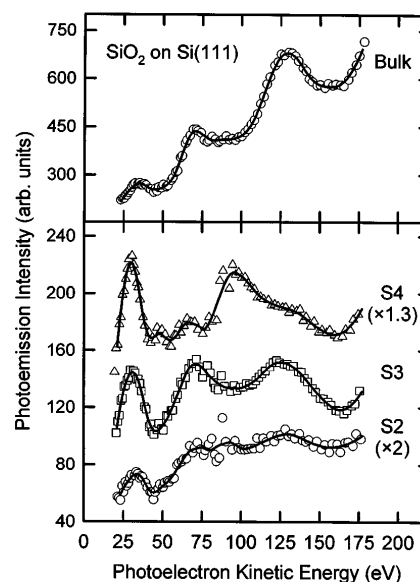


FIG. 2. Photoemission intensities of the bulk component (top panel) and the S2–S4 components (bottom panel) as a function of photoelectron kinetic energy. Dashed lines show the smooth backgrounds which were subtracted to obtain the  $\chi$  functions. These background functions were obtained by smoothing the data using a quadratic Loess function.

cal path length difference, the diffraction oscillations are dominated by backscattering from atoms located directly behind the emitter, at a path length difference of  $2kR$ . Our calculation shows that the intensity for each sidescattering in bulk Si is no more than  $\sim 3\%$  of the backscattering intensity. PEFS, in our case, then acts like a vector-EXAFS (extended x-ray-absorption fine structure) technique, measuring bond lengths only in the  $-z$  direction. Specifically, we are sensitive to the interlayer bond length, and whether or not this bond has an O atom inserted into it. However, if the emitter is in a disordered state such that the bond axes are randomly oriented, all of the nearest neighbors will contribute, and the resulting signal will be similar, but not exactly equivalent, to EXAFS.

As is done in standard PEFS analyses, the oscillatory part of the intensity variation in Fig. 2 is extracted for each oxidation state to obtain the so-called  $\chi$  function. These  $\chi$  functions are Fourier transformed with respect to the path length difference to obtain the bond length distribution functions,

$$F(R) = \int_{k_{\min}}^{k_{\max}} \chi(k) e^{i2kR} g(k) k dk,$$

where  $g(k)$  is a window function. The results are shown in Fig. 3. The two vertical dashed lines in Fig. 3 mark the Si-O and Si-Si bond lengths, corrected for the appropriate backscattering and forward-scattering phase shifts [9,10]. Clearly, the bond lengths measured for bulk Si and for S4 ( $\text{Si}^{4+}$ ) are in excellent agreement with the Si-Si bond length and Si-O bond length, respectively. This is exactly what we expect, because, for bulk Si, there are only Si

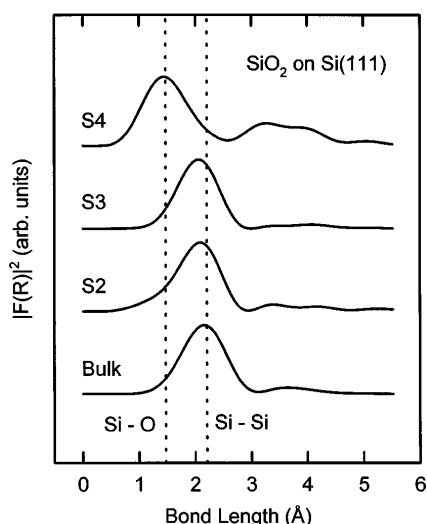


FIG. 3. The bond-length distributions for  $\text{SiO}_x/\text{Si}(111)$ . Vertical dotted lines indicate the expected Si-O and Si-Si bond lengths, corrected for the scattering phase shifts.

nearest neighbors behind the emitter, while for S4, which corresponds to Si in the amorphous  $\text{SiO}_2$  layer, there are only O nearest neighbors. The intermediate oxidation states S2 and S3, corresponding to Si in suboxides, show essentially pure Si-Si bonding. These results indicate that the S2 and S3 emitters are bonded primarily to Si in the  $-z$  direction. Such an orientational effect has a significant implication concerning the bonding structure of the suboxide species. If the suboxides were disordered as is S4 in amorphous  $\text{SiO}_2$ , we would expect to see a much shorter average bond length, especially in the case of S3, which is bonded to three O atoms and only one Si atom. The S2 and S3 emitters must then be oriented at the interface with Si nearest neighbors in the  $-z$  direction.

A chemically graded, amorphous oxide film with distributed suboxide species is thus inconsistent with our finding. Our results can only be explained by assigning S2 and S3 to  $\text{Si}^{2+}$  and  $\text{Si}^{3+}$  confined to a chemically abrupt interface between Si and  $\text{SiO}_2$ . Figure 4 is a simple schematic diagram showing the atomic bonding geometry, where the horizontal dashed line indicates the abrupt boundary between Si and  $\text{SiO}_2$ . Just below this boundary, each Si atom terminating the Si(111) substrate lattice has either one or three bonds extending to the  $\text{SiO}_2$  side (three bonds for intrabilayer termination, and one bond for interbilayer termination). These bonds can be joined to either Si or O on the side of the  $\text{SiO}_2$ , as indicated by the various possible configurations in the figure. Clearly, all of the suboxide species are either just above or just below the boundary, and the backbond of every  $\text{Si}^{2+}$  and  $\text{Si}^{3+}$  in the  $-z$  direction is to a Si atom, which is what our experimental results indicate. Our finding is, however, in opposition to a previous model based on an x-ray photoelectron intensity analysis, in which  $\text{Si}^{3+}$  is thought to be distributed throughout the thin  $\text{SiO}_2$  layer [1]. This discrepancy might be related

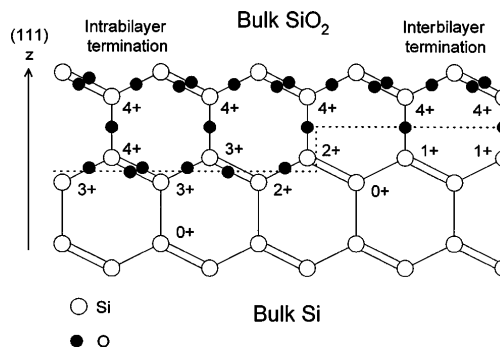


FIG. 4. An abrupt interface model for  $\text{SiO}_2/\text{Si}(111)$ . There are two possible terminations, as indicated in the figure. The oxidation states for Si atoms at and near the interface boundary are labeled.

to the different sample preparation procedures employed in that study (the presence of H and OH species from wet chemical processing may affect the stoichiometry of the  $\text{SiO}_2$  layer; for example, a Si bond could be terminated by a H atom within the  $\text{SiO}_2$  layer).

Our results also have implications for the interface growth model. The observation of a chemically abrupt interface implies that there are no partially oxidized bilayers with the interbilayer substrate bond filled, suggesting that the bilayer must be fully oxidized before proceeding to fill the interbilayer bonds. This is in agreement with recent electron microscopy results which show that the thermal oxidation of Si(111) proceeds by the reaction of discrete monolayers with no flow of surface steps [11]. This implies a layer-by-layer oxidation mechanism, which is consistent with our observation of a chemically abrupt interface.

In summary, we have made the first direct measurements of the intermediate oxidation state bonding at the  $\text{SiO}_2/\text{Si}(111)$  interface. Our results show evidence for a chemically abrupt interface, with the suboxide states confined to the interface.

The authors would like to thank J. Murray Gibson for several illuminating conversations. This material is based upon work supported by the Division of Materials Sciences, Office of Basic Energy Sciences, U.S. Department of Energy, under Grant No. DEFG02-91ER45439. Acknowledgment is also made to the Donors of the Petroleum Research Fund, administered by the American Chemical Society, and to the U.S. National Science Foundation (Grant No. DMR-92-23546) for partial support of the synchrotron beamline operation and personnel. The Synchrotron Radiation Center of the University of Wisconsin is supported by the National Science Foundation.

\*Present address: Environmental Molecular Sciences Laboratory, Pacific Northwest National Laboratory, P.O. Box 999, MSIN K2-14, Richland, WA 99352.

<sup>†</sup>To whom correspondence should be addressed.  
Electronic address: t-chiang@uiuc.edu

- [1] P. J. Grunthaner, M. H. Hecht, F. J. Grunthaner, and N. M. Johnson, *J. Appl. Phys.* **61**, 629 (1987); F. J. Grunthaner and P. J. Grunthaner, *Mater. Sci. Rep.* **1**, 65 (1986).
- [2] A. Munkholm, S. Brennan, F. Comin, and L. Ortega, *Phys. Rev. Lett.* **75**, 4254 (1995). An ordered component was observed, but with a concentration less than 1%.
- [3] G. Hollinger and F. J. Himpsel, *J. Vac. Sci. Technol. A* **1**, 640 (1983); *Phys. Rev. B* **28**, 3651 (1983); *Appl. Phys. Lett.* **44**, 93 (1984); F. J. Himpsel, F. R. McFeely, A. Taleb-Ibrahimi, J. A. Yarmoff, and G. Hollinger, *Phys. Rev. B* **38**, 6084 (1988).
- [4] S. Iwata and A. Ishizaka, *J. Appl. Phys.* **79**, 6653 (1996).
- [5] M. M. B. Holl and F. R. McFeely, *Phys. Rev. Lett.* **71**, 2441 (1993). These authors proposed a different interpretation for the chemical shifts, but this alternate interpretation was not supported by a recent calculation [A. Pasquarello, M. S. Hybertsen and R. Car, *Phys. Rev. Lett.* **74**, 1024 (1995)].
- [6] V. Fritzsche and D. P. Woodruff, *Phys. Rev. B* **46**, 16 128 (1992); J. A. Carlisle, M. T. Sieger, T. Miller, and T.-C. Chiang, *Phys. Rev. Lett.* **71**, 2955 (1993); P. S. Mangat, K. M. Choudhary, D. Kilday, and G. Margaritondo, *Phys. Rev. B* **44**, 6284 (1991), P. S. Mangat, P. Soukiassian, K. M. Schirm, L. Spiess, S. P. Tang, A. J. Freeman, Z. Hurych and B. Delley, *Phys. Rev. B* **47**, 16 311 (1993).
- [7] P. A. Lee, P. H. Citrin, P. Eisenberger, and B. M. Kincaid, *Rev. Mod. Phys.* **53**, 769 (1981).
- [8] J. J. Barton, S. W. Robey, and D. A. Shirley, *Phys. Rev. B* **34**, 778 (1986).
- [9] P. Vashishta, R. K. Kalia, J. P. Rino, and I. Ebbsjö, *Phys. Rev. B* **41**, 12 197 (1990).
- [10] M. T. Sieger, D. H. Madison, and T.-C. Chiang (unpublished).
- [11] F. M. Ross and J. M. Gibson, *Phys. Rev. Lett.* **68**, 1782 (1992).